



Cite this: DOI: 10.1039/d5cc01017a

Received 25th February 2025,
Accepted 9th April 2025

DOI: 10.1039/d5cc01017a

rsc.li/chemcomm

From LCST to crystals: structural modulation of ionic liquids drives the phase transition of poly(2-isopropyl-2-oxazoline)[†]

Mai Kamiyama-Ueda, ^{‡ab} Takeshi Ueki, ^{‡*ab} Yuji Kamiyama, ^a
Ryota Tamate, ^a Keisuke Watanabe ^c and Yukiteru Katsumoto ^{*c}

Poly(2-isopropyl-2-oxazoline) (PiPrOx) exhibits UCST- or LCST-type phase transitions in ionic liquids (ILs) depending on the IL structure. In LCST-type ILs, where low solution entropy is favorable, PiPrOx crystallizes immediately after phase separation, unlike in water. FT-IR reveals a *trans*-rich conformation with structural constraint, facilitating both LCST-type phase separation and rapid crystallization.

Polymer crystallization from solution is a cornerstone process in materials science, underpinning diverse industrial applications such as functional membrane productions and wet spinning for fibers. The choice of solvent critically impacts the crystallization process, dictating crystal morphology, growth kinetics and the resulting material properties.^{1,2} Among various solvent systems, ionic liquids (ILs) have emerged as highly versatile candidates for polymer processing due to their unique properties,³ including negligible vapor pressure, high thermal stability, and the ability to dissolve a wide range of polymers.^{4–7} Beyond these advantages, the structural tunability of ILs offers unparalleled flexibility to design solvent environments tailored for phase behavior of polymers.^{8–13} This structural tunability and environmental sustainability positions ILs as a promising platform for advancing polymer crystallization and applications. Herein, we reveal the phase behaviors and crystallization dynamics of poly(2-isopropyl-2-oxazoline) (PiPrOx) in imidazolium-based ILs. PiPrOx is a unique polymer that

exhibits lower critical solution temperature (LCST)-type phase behavior in aqueous solutions, where it undergoes slow crystallization through prolonged annealing after phase separation.^{14–17} Structurally, PiPrOx is an isomer of poly(*N*-isopropylacrylamide) (PNiPAm), the most widely studied LCST-type polymer in water. PNiPAm is also known to exhibit opposite upper critical solution temperature (UCST)-type phase behavior in ILs^{18–21} (Fig. 1). PiPrOx demonstrates both UCST- and

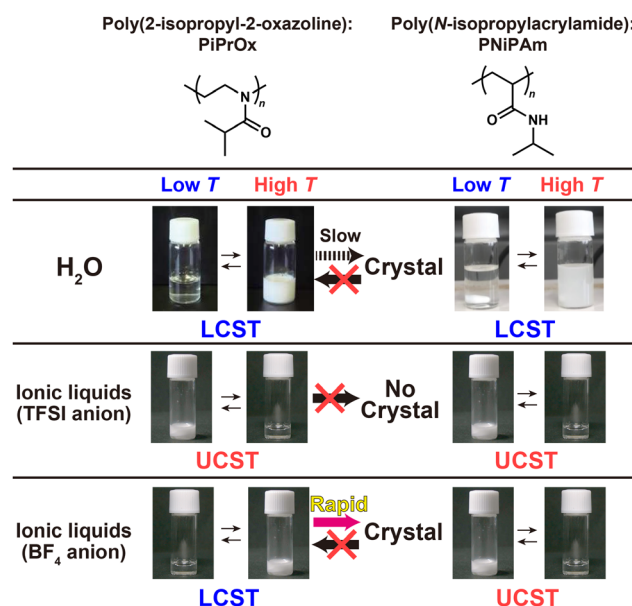


Fig. 1 Chemical structure of poly(2-isopropyl-2-oxazoline) (PiPrOx) and poly(*N*-isopropylacrylamide) (PNiPAm) and their phase behaviors in water and ionic liquids (ILs). PiPrOx exhibits LCST-phase transitions in water, followed by slow crystallization upon prolonged heating. In ILs, PiPrOx demonstrates UCST- and LCST-type phase transitions, depending on the IL structure, with rapid crystallization observed immediately after LCST-type phase separation in BF₄-based ILs. By contrast, PNiPAm undergoes LCST-type transitions in water and exclusively UCST-type transitions in ILs, without exhibiting crystallization.

^a Research Centre for Macromolecules and Biomaterials,
National Institute of Materials and Science, 1-1 Namiki, Tsukuba,
Ibaraki 305-0044, Japan. E-mail: UEKI.Takeshi@nims.go.jp

^b Graduate School of Life Science, Hokkaido University, Kita 10, Nishi 8, Kita-ku,
Sapporo, Hokkaido 060-0810, Japan

^c Department of Chemistry, Faculty of Science, Fukuoka University,
8-19-1 Nanakuma, Johnan-ku, Fukuoka 814-0180, Japan.
E-mail: katsumoto@fukuoka-u.ac.jp

[†] Electronic supplementary information (ESI) available: Experimental details,
GPC traces, and thermodynamic aspects of the phase transition of polymers in
ILs. See DOI: <https://doi.org/10.1039/d5cc01017a>

[‡] M. K.-U. and T. U. contributed equally.



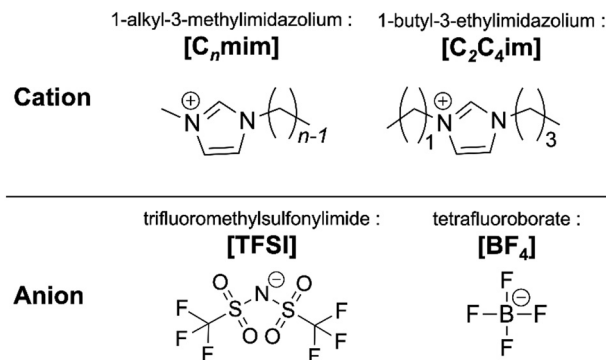


Fig. 2 Chemical structures and names of the cations and anions of the ILs used in this study. The cations include 1-alkyl-3-methylimidazolium ([C_nmim]) and 1-butyl-3-ethylimidazolium ([C₂C₄im]), while the anions consist of trifluoromethylsulfonylimide ([TFSI]) and tetrafluoroborate ([BF₄]).

LCST-type phase behaviors, depending on the anion structure of the IL. Specifically, PiPrOx transitions *via* a UCST-type phase separation in [C_nmim][TFSI] systems, while LCST-type phase separation are observed in 1-hexyl-3-methylimidazolium tetrafluoroborate ([C₆mim][BF₄]) and in 1-butyl-3-ethylimidazolium tetrafluoroborate ([C₂C₄im][BF₄]) (Fig. 2). In only the latter case, PiPrOx undergoes rapid crystallization immediately following LCST-type phase separation—a phenomenon sharply contrasting the slower crystallization observed in aqueous solutions. FT-IR spectroscopy revealed that PiPrOx adopts a *trans*-rich conformation when dissolved in LCST-type ILs, effectively rendering the polymer 'ready-to-crystallize'.

We initially screened the solubility of PiPrOx in 43 kinds of ILs, covering a temperature range from 4 °C to 120 °C (Table S1 in the ESI†). Among these, ILs containing [BF₄] and trifluoromethylsulfonylimide ([TFSI]) anions were selected. A detailed rationale for this selection is available in the ESI.† Fig. 3 shows the transmittance curve for the PiPrOx (*M_n* = 7700 g mol^{−1}, *M_w*/*M_n* = 1.30) in [C₆mim][BF₄] and [C₂C₄im][BF₄], respectively. We found that the PiPrOx exhibited LCST-type phase separation both in [C₆mim][BF₄] and [C₂C₄im][BF₄]. Table 1 compares the solubility of PiPrOx and PNIPAm in ILs. PiPrOx exhibited LCST-type phase separation in [C₆mim][BF₄] and [C₂C₄im][BF₄], while PiPrOx showed UCST-type phase separation in [C₂mim][TFSI] and [C₄mim][TFSI]. In contrast, PNIPAm showed only

UCST-type phase separation in both [C_nmim][BF₄] with an alkyl carbon number in the imidazolium cation of *n* = 2, 3 or 4 and [C_nmim][TFSI] with *n* = 2, 4, 6, 8, 10 and 12. Fig. 4(a) shows the relationship between the *T_c*, defined as the temperature corresponding to 50% transmittance, of the polymers (2 wt% in ILs) and *n* of the imidazolium cation. It is revealed that the UCST-type phase separation temperature (*T_{c,u}*) monotonically decreases with an increase in alkyl chain length. It is widely reported that the mutual solubility in ILs improves as the length of the alkyl chain attached to the cation increases both in UCST-^{22,23} and LCST-systems.^{24,25} A solubility improvement of the polymer following an increase in the alkyl chain length has also been reported in certain LCST-type phase separations of polymethacrylates^{11,13,26} and polyethers.^{12,20,27} A similar tendency was observed to increase the *T_{c,u}* of the present system. As can be seen in Table 1 and Fig. 4(a), LCST-type phase separation of PiPrOx occurred only when [C₆mim][BF₄] was used as the solvent. PiPrOx was incompatible with [C_nmim][BF₄] at *n* = 2, 3, and 4, and gave a completely compatible system at *n* = 8. This also indicates that extending the alkyl chain length works to increase solubility.

Fig. 4(b) highlights the phase separation temperature of PiPrOx and PNIPAm in [C₄mim][BF₄], [C₆mim][BF₄], and [C₂C₄im][BF₄] as solvents. For [C₂C₄im][BF₄], where the cation carries four carbons (butyl group) at position 1 and two carbons (ethyl group) at position 3, the solubility of PiPrOx is lower compared to [C₆mim][BF₄], which carries six carbons (hexyl group) only at position 3. Consequently, the LCST-type phase separation temperature of PiPrOx in [C₂C₄im] is nearly 30 °C lower than that in [C₆mim][BF₄]. In contrast, the UCST-type phase separation temperature of PNIPAm decreases by only 2 °C when the cation changes from [C₂C₄im] to [C₆mim]. The greater shift observed in the LCST-type phase separation temperature compared to the UCST-type phase separation temperature suggests that the introduction of alkyl chains at both positions 1 and 3 of the imidazolium ring significantly impacts the thermodynamics of the solution. Detailed discussions on the phase behavior of PiPrOx and PNIPAm in ILs from thermodynamic aspects are available in the ESI.†

Previous work demonstrated that PiPrOx exhibited LCST-type phase separation in aqueous solution, similar to PNIPAm. However, unlike PNIPAm, PiPrOx undergoes crystallization in the polymer-rich phase after prolonged heating. In water, the crystallization of PiPrOx follows LCST-type phase separation. At temperatures above the phase transition, polymer-rich droplets form, initially smooth but slowly transforming into rugged crystalline structures upon prolonged heating.²⁸ The process requires ~20 hours at *T_c* + 2 °C, indicating slow kinetics. PiPrOx chains must overcome rotational energy barriers in the backbone C–C and C–N bonds to adopt the *trans*-conformation needed for crystallization. Prior studies revealed that PiPrOx can be kinetically trapped in metastable *gauche*-conformers before reaching the most energetically favorable *trans*-conformer, making conformational alignment a rate-determining step for nucleation.²⁸ We discovered that PiPrOx crystallizes rapidly in IL systems, immediately after undergoing LCST-type phase separation. Notably, after cooling the

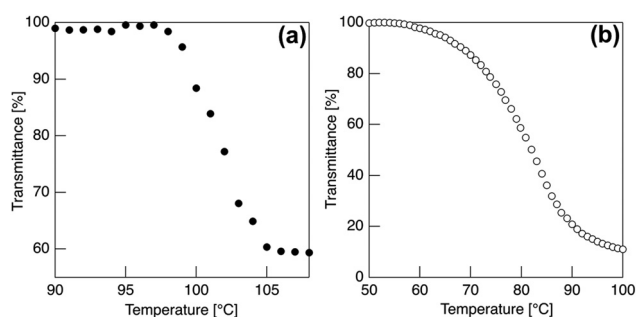


Fig. 3 Transmittance curves of PiPrOx in (a) [C₆mim][BF₄] and (b) [C₂C₄im][BF₄].



Table 1 Summary of the solubility test for the PiPrOx and PNIPAm in $[C_n\text{mim}][\text{BF}_4]$, $[C_n\text{mim}][\text{TFSI}]$, and $[\text{C}_2\text{C}_4\text{im}][\text{BF}_4]$. Polymer concentration is 2 wt%. "Yes" and "No" mean the combination gives compatible and incompatible systems, respectively. The temperature conditions are from 4 °C to 120 °C

Anion: [TFSI]	C ₂ mim		C ₄ mim		C ₆ mim	C ₈ mim	C ₁₀ mim	C ₁₂ mim
PiPrOx	UCST		UCST		Yes	Yes	Yes	Yes
PNiPAm	UCST		UCST		UCST	UCST	UCST	UCST
Anion: [BF ₄]	C ₂ mim	C ₃ mim	C ₄ mim	C ₂ C ₄ im	C ₆ mim	C ₈ mim	C ₁₀ mim	
PiPrOx	No	No	No	LCST	LCST	Yes	Yes	
PNiPAm	UCST	UCST	UCST	UCST	Yes	Yes	Yes	

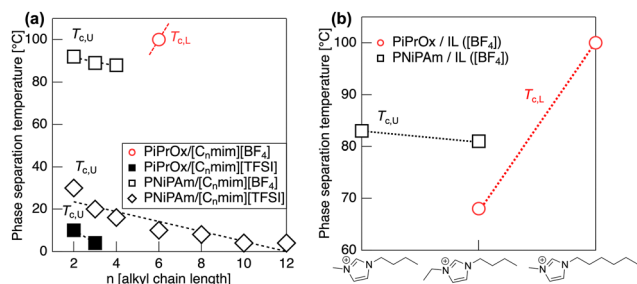


Fig. 4 (a) Relationship between phase transition temperature and alkyl chain length of the imidazolium cation. (b) Phase transition temperature of PiPrOx and PNIPAm in $[\text{C}_4\text{mim}][\text{BF}_4]$, $[\text{C}_2\text{C}_4\text{im}][\text{BF}_4]$, and $[\text{C}_6\text{mim}][\text{BF}_4]$ as solvents.

solution following LCST-type phase separation, the solution did not return to its original transparent state. Further investigation revealed that the polymer-rich phase, once washed with methanol, was insoluble, and microscopic analysis of the precipitate confirmed the formation of crystals (Fig. 5(A)). In other PiPrOx/IL combinations exhibiting UCST-type phase separations, the polymer-rich phase precipitated at low temperatures did not show any detectable crystallization under the same experimental conditions. FT-IR measurements revealed that the rapid crystallization of PiPrOx is attributed to its molecular conformation in $[\text{C}_6\text{mim}][\text{BF}_4]$ (Fig. 5(B)). The C–N stretching band between 1400 and 1450 cm^{-1} indicates the *trans*-rich conformation of PiPrOx, confirmed by DFT calculations with model compounds. In the FT-IR spectrum of PiPrOx dissolved in $[\text{C}_6\text{mim}][\text{BF}_4]$ (Fig. 5(B)(d)), the C–N stretching

band shows high intensity, suggesting a *trans*-rich conformation even in the dissolved state. In contrast, the FT-IR spectrum of PiPrOx aqueous solution exhibits weaker C–N stretching band intensity (Fig. 5(B)(a)). This indicates that the transformation toward a *trans*-rich conformation occurs gradually (Fig. 5(B)(b)), contributing to slower crystallization. The inherent *trans*-rich conformation in the ILs closely resembles its crystalline state (Fig. 5(B)(c)), lowering the energetic barrier for crystallization and facilitating rapid crystal formation after LCST-type phase separation. By contrast, in aqueous systems, PiPrOx requires significant conformational adjustments post-phase separation, delaying crystallization onset. In UCST systems such as PiPrOx in $[\text{C}_2\text{mim}][\text{TFSI}]$, the FT-IR spectra confirm no *trans*-rich conformation in the dissolved state (Fig. S6 and S7, ESI†). This lack of pre-alignment likely explains the absence of crystallization in UCST-type phase separations and underscores the critical role of the *trans*-rich conformation in facilitating rapid crystallization in LCST-type phase separation systems. A noteworthy aspect of the *trans*-rich PiPrOx conformer is its potential influence on solution entropy. This conformational restriction may reduce mixing entropy, serving as a thermodynamic requirement of LCST-type phase separation. This interpretation agrees with the lack of crystallization in UCST-type PiPrOx/IL systems, where phase transitions do not rely on entropy-lowering solvation. To further explore the structural origin of the *trans*-rich state, we examined the conformation of PiPrOx in $[\text{C}_6\text{mim}][\text{TFSI}]$ and $[\text{C}_8\text{mim}][\text{BF}_4]$ (Fig. S8, ESI†). The latter, despite being fully miscible, shows strong C–N stretching bands similar to $[\text{C}_6\text{mim}][\text{BF}_4]$, whereas $[\text{C}_6\text{mim}][\text{TFSI}]$ exhibits much weaker intensity. This suggests that the $[\text{BF}_4]$ anion plays a key role in stabilizing the *trans*-conformation. The absence of LCST behavior in $[\text{C}_8\text{mim}][\text{BF}_4]$, despite the *trans*-rich state, is likely due to enhanced polymer-solvent interactions caused by longer alkyl chains, elevating the LCST above the experimental range. Furthermore, to assess differences among $[\text{BF}_4]$ -based ILs, we compared IR spectra of PiPrOx in $[\text{C}_6\text{mim}][\text{BF}_4]$ and $[\text{C}_2\text{C}_4\text{im}][\text{BF}_4]$ (Fig. S9, ESI†). Both display comparable C–N band intensities, indicating that the *trans*-rich conformation exists in both. Therefore, the ~ 30 °C difference in LCST-type transition temperature between them likely arises not from differences in the conformation, but from a dissimilarity in solvation-related factors, potentially linked to the degree of nanostructuring in longer-chain ILs like $[\text{C}_6\text{mim}][\text{BF}_4]$. Finally, we note that the *trans*-rich conformation observed in ILs may reduce not only the conformational

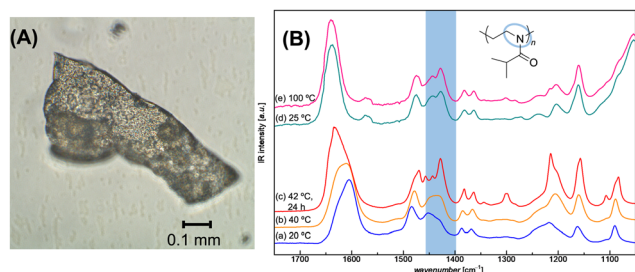


Fig. 5 (A) A photograph of the PiPrOx crystal deposited from $[\text{C}_6\text{mim}][\text{BF}_4]$. (B) FT-IR spectra of PiPrOx (a) in D_2O homogeneous solution before phase transition, (b) soon after phase separation from D_2O , (c) after complete phase separation from D_2O , (d) in $[\text{C}_6\text{mim}][\text{BF}_4]$ homogeneous solution before phase transition, and (e) soon after phase separation from $[\text{C}_6\text{mim}][\text{BF}_4]$.

entropy but also the configurational entropy, as the spatial freedom in the configuration of the extended chains should be highly limited compared to that of flexible random coils. This dual entropy reduction could serve as an additional driving force for the LCST-type phase separation.

In this study, we described the unique phase transition behaviors of PiPrOx in ILs, revealing its ability to exhibit either UCST- or LCST-type phase separation depending on the IL structure. The rapid crystallization of PiPrOx in ILs, observed immediately after LCST-type phase separation, marked a significant departure from the slow crystallization kinetics in aqueous systems. Our findings unveil novel insights into polymer-IL interactions, emphasizing the role of IL structure in modulating polymer phase behavior and offering a foundation for designing advanced functional materials.

This study was financially supported by JSPS KAKENHI grants (20H02804, 20K21229, and 23H02030 to T. U.). T. U. thanks Sadaki Samitsu for fruitful discussion on the crystallization of the polymer.

Data availability

The data supporting this article have been included as part of the ESI.†

Conflicts of interest

There are no conflicts to declare.

Notes and references

- 1 B. Wunderlich, *Macromolecular Physics*, Academic Press, New York, 1973.
- 2 L. Mandelkern, *Crystallization of Polymers*, Cambridge University Press, Cambridge, 2004.
- 3 N. V. Plechkova and K. R. Seddon, *Chem. Soc. Rev.*, 2008, 37, 123–150.
- 4 S. Singh, B. A. Simmons and K. P. Vogel, *Biotechnol. Bioeng.*, 2009, 104, 68–75.
- 5 S. Zhu, Y. Wu, Q. Chen, Z. Yu, C. Wang, S. Jin, Y. Ding and G. Wu, *Green Chem.*, 2006, 8, 325–327.
- 6 H. Xie, S. Li and S. Zhang, *Green Chem.*, 2005, 7, 606.
- 7 S. S. Silva, T. C. Santos, M. T. Cerqueira, A. P. Marques, L. L. Reys, T. H. Silva, S. G. Caridade, J. F. Mano and R. L. Reis, *Green Chem.*, 2012, 14, 1463–1470.
- 8 N. Winterton, *J. Mater. Chem.*, 2006, 16, 4281.
- 9 R. Tamate and T. Ueki, *Chem. Rec.*, 2023, 23, e202300043.
- 10 T. Ueki, *Polym. J.*, 2014, 46, 646–655.
- 11 T. Ueki and M. Watanabe, *Langmuir*, 2007, 23, 988–990.
- 12 H. N. Lee and T. P. Lodge, *J. Phys. Chem. Lett.*, 2010, 1, 1962–1966.
- 13 H. N. Lee and T. P. Lodge, *J. Phys. Chem. B*, 2011, 115, 1971–1977.
- 14 R. Luxenhofer, Y. Han, A. Schulz, J. Tong, Z. He, A. V. Kabanov and R. Jordan, *Macromol. Rapid Commun.*, 2012, 33, 1613–1631.
- 15 T. Lorson, M. M. Lubtow, E. Wegener, M. S. Haider, S. Borova, D. Nahm, R. Jordan, M. Sokolski-Papkov, A. V. Kabanov and R. Luxenhofer, *Biomaterials*, 2018, 178, 204–280.
- 16 C. Weber, R. Hoogenboom and U. S. Schubert, *Prog. Polym. Sci.*, 2012, 37, 686–714.
- 17 T. Chung, J. Han, Y. J. Kim, K.-J. Jeong, J. M. Koo, J. Lee, H. G. Park, T. Joo and Y. S. Kim, *Polym. Chem.*, 2022, 13, 4615–4624.
- 18 T. Ueki and M. Watanabe, *Chem. Lett.*, 2006, 35, 964–965.
- 19 H. Asai, K. Fujii, T. Ueki, S. Sawamura, Y. Nakamura, Y. Kitazawa, M. Watanabe, Y.-S. Han, T.-H. Kim and M. Shibayama, *Macromolecules*, 2013, 46, 1101–1106.
- 20 H.-N. Lee, Z. Bai, N. Newell and T. P. Lodge, *Macromolecules*, 2010, 43, 9522–9528.
- 21 S. So and R. C. Hayward, *ACS Appl. Mater. Interfaces*, 2017, 9, 15785–15790.
- 22 J. M. Crosthwaite, S. N. V. K. Aki, E. J. Maginn and J. F. Brennecke, *J. Phys. Chem. B*, 2004, 108, 5113–5119.
- 23 J. M. Crosthwaite, M. J. Muldoon, S. N. V. K. Aki, E. J. Maginn and J. F. Brennecke, *J. Phys. Chem. B*, 2006, 110, 9354–9361.
- 24 J. Łachwa, J. Szydlowski, A. Makowska, K. R. Seddon, J. M. S. S. Esperança, H. J. R. Guedes and L. P. N. Rebelo, *Green Chem.*, 2006, 8, 262.
- 25 J. Łachwa, J. Szydlowski, V. Najdanovic-Visak, L. P. N. Rebelo, K. R. Seddon, M. N. da Ponte, J. M. S. S. Esperança and H. J. R. Guedes, *J. Am. Chem. Soc.*, 2005, 127, 6542–6543.
- 26 K. Kodama, H. Nanashima, T. Ueki, H. Kokubo and M. Watanabe, *Langmuir*, 2009, 25, 3820–3824.
- 27 K. Kodama, R. Tsuda, K. Niitsuma, T. Tamura, T. Ueki, H. Kokubo and M. Watanabe, *Polym. J.*, 2011, 43, 242–248.
- 28 Y. Katsumoto, A. Tsuchiizu, X. Qiu and F. M. Winnik, *Macromolecules*, 2012, 45, 3531–3541.

